De Novo Variants in SPOP Cause Two Clinically Distinct Neurodevelopmental Disorders

Maria J. Nabais Sá,[1] Geniver El Tekle,[2,3,4] Arjan P.M. de Brouwer,[1] Sarah L. Sawyer,[5] Daniela del Gaudio,[6] Michael J. Parker,[7] Farah Kanani,[7] Marie-José H. van den Boogaard,[8] Koen van Gassen,[8] Margot I. Van Allen,[9] Klaas Wierenga,[10] Gabriela Purcarin,[10] Ellen Roy Elias,[11,12] Amber Begtrup,[13] Jennifer Keller-Ramey,[13] Tiziano Bernasocchi,[2,3,4] Laurens van de Wiel,[14] Christian Gilissen,[15] Hanka Venselaar,[14] Rolph Pfundt,[1] Lisenka E.L.M. Vissers,[1] Jean-Philippe P. Theurillat,[2,3,16,*] and Bert B.A. de Vries[1,16,*]

Recurrent somatic variants in SPOP are cancer specific; endometrial and prostate cancers result from gain-of-function and dominant-negative effects toward BET proteins, respectively. By using clinical exome sequencing, we identified six de novo pathogenic missense variants in SPOP in seven individuals with developmental delay and/or intellectual disability, facial dysmorphisms, and congenital anomalies. Two individuals shared craniofacial dysmorphisms, including congenital microcephaly, that were strikingly different from those of the other five individuals, who had (relative) macrocephaly and hypertelorism. We measured the effect of SPOP variants on BET protein amounts in human Ishikawa endometrial cancer cells and patient-derived cell lines because we hypothesized that variants would lead to functional divergent effects on BET proteins. The de novo variants c.362G>A (p.Arg121Gln) and c. 430G>A (p.Asp144Asn), identified in the first two individuals, resulted in a gain of function, and conversely, the c.73A>G (p.Thr25Ala), c.248A>G (p.Tyr83Cys), c.395G>T (p.Gly132Val), and c.412C>T (p.Arg138Cys) variants resulted in a dominant-negative effect. Our findings suggest that these opposite functional effects caused by the variants in SPOP result in two distinct and clinically recognizable syndromic forms of intellectual disability with contrasting craniofacial dysmorphisms.

Pathogenic variants in a considerable number of highly mutable genes lead to cancer when they occur in somatic cells, and they can lead to neurodevelopmental disorders (NDD) if occur in the germline or early in the embryonic development.[1] They frequently disrupt normal cell proliferation and/or differentiation while evading cellular death. Moreover, mutational hotspots in both somatic cell lines and germlines point toward analogous functional effects of pathogenic variants. Examples include gain-of-function variants in genes of the RAS-MAP kinase pathway, such as PTPN11,[2,3] and loss-of-function variants in several genes of pathways that regulate chromatin remodeling, such as ASXL1.[4–6] Nevertheless, recognizing the clinical relevance and investigating the functional impact of de novo missense mutations in genes associated with NDD remains challenging. By using in silico and in vitro analyses, we examined the effect of de novo clustered missense SPOP variants identified in individuals with NDD on protein interactions.

SPOP (MIM: 602650) encodes the speckle-type POZ (pox virus and zinc finger protein; SPOP) protein in humans.

SPOP homodimers function as a substrate adaptor of a larger cullin3-RING-based ubiquitin ligase complex that mediates the ubiquitination of target proteins; this ubiquitination usually leads to proteasomal degradation of the proteins.[7] SPOP contains an evolutionarily conserved meprin and tumor necrosis factor (TNF)-receptor associated factor (TRAF) homology (MATH) domain; a bric-a-brac, tramtrack, and broad complex (BTB) domain (also known as a POZ domain); a three-box domain; and a C-terminal nuclear localization sequence.[8,9] The MATH domain mediates interaction with protein-ubiquitin ligase substrates, such as BRD2, BRD3, and BRD4 proteins, which are collectively referred to as BETs.[10]

Somatic missense SPOP variants restricted to the MATH domain are frequently identified in prostate cancer[11,12] and endometrial cancer.[10,13] Indeed, with up to 6–15% of localized prostate tumors harboring acquired heterozygous missense SPOP variants, SPOP is the most commonly point-mutated gene in prostate cancer.[12] These missense SPOP variants act in a dominant-negative fashion to repress ubiquitination and degradation of oncogenic

[1]Department of Human Genetics, Donders Institute for Brain, Cognition and Behavior, Radboud University Medical Center, 6525 GA Nijmegen, the Netherlands; [2]Functional Cancer Genomics, Institute of Oncology Research, 6500 Bellinzona, Switzerland; [3]Faculty of Biomedical Science, Università della Svizzera Italiana, 6900 Lugano, Switzerland; [4]University of Lausanne, 1015 Lausanne, Switzerland; [5]Department of Genetics, Children's Hospital of Eastern Ontario and Children's Hospital of Eastern Ontario Research Institute, University of Ottawa, Ottawa, ON K1H 8L1, Canada; [6]Molecular Diagnostic Laboratory, Department of Human Genetics, University of Chicago, Chicago, IL 60637, USA; [7]Department of Clinical Genetics, Sheffield Children's NHS Foundation Trust, Sheffield S10 2TH, UK; [8]Department of Genetics, UMC Utrecht, 3584 CX Utrecht, the Netherlands; [9]Department of Medical Genetics, University of British Columbia, Vancouver, BC V6H 3N1, Canada; [10]University of Oklahoma Health Sciences Center, Oklahoma City, OK 73104, USA; [11]Special Care Clinic, Children's Hospital Colorado, Aurora, CO 80011, USA; [12]University of Colorado School of Medicine, Aurora, CO 80045, USA; [13]GeneDx, Gaithersburg, MD 20877, USA; [14]Center for Molecular and Biomolecular Informatics, Radboud Institute for Molecular Life Sciences, Radboud University Medical Center, 6525 GA Nijmegen, the Netherlands; [15]Department of Human Genetics, Radboud Institute for Molecular Life Sciences, Radboud University Medical Center, 6525 GA Nijmegen, the Netherlands
[16]These authors contributed equally to this work
*Correspondence: jean-philippe.theurillat@ior.usi.ch (J.-P.P.T.), bert.devries@radboudumc.nl (B.B.A.d.V.)
https://doi.org/10.1016/j.ajhg.2020.02.001.
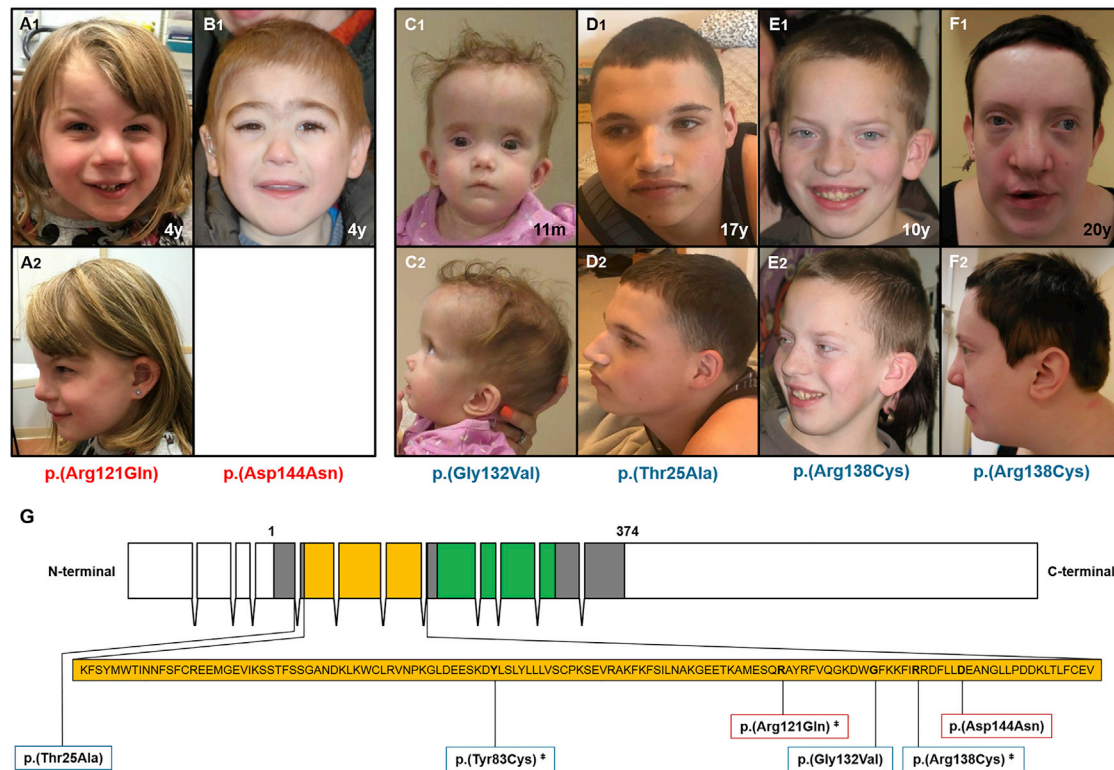© 2020 American Society of Human Genetics.

Figure 1. Craniofacial Dysmorphisms of Individuals and Their Respective *De Novo* Variants in *SPOP*

(A–F) Individuals 1 (A) and 2 (B) had microcephaly, a round face, prominent glabella, a depressed nasal bridge, narrow palpebral fissures, a short nose with anteverted nares, micrognathia, and/or a pointed chin. Individuals 3 (C), 4 (D), 5 (E), and 6 (F) had macrocephaly, a long face, a high anterior hairline, a high forehead, widely spaced eyes, a prominent and wide nasal bridge, a wide and bulbous nasal tip, underdeveloped nasal alae, and/or low-hanging columella.

(G) *SPOP* mRNA with 12 exons (GenBank: NM_001007226.1; residues 1–374 correspond to the coding sequence, in grey), including the MATH domain, represented in yellow (residues 31–161) and the BTB domain (also called a POZ domain) represented in green (residues 173–297) (GenBank: NP_001007227.1; Uniprot: O43791). Affected amino acid residues are printed in bold. Variants eliciting a gain of function are noted in red; dominant-negative variants are noted in blue. *SPOP* variants marked with ‡ were identified in both germlines and somatic cell lines, as described in Table S2.

substrate proteins.[14–17] In contrast, recurrent missense *SPOP* variants in endometrial cancer result in a SPOP gain of function leading to enhanced degradation of distinct protein substrates, including the BET proteins.[10]

Two unrelated individuals with the same *de novo SPOP* variant were identified via trio-based clinical exome sequencing. One was in a cohort of 4,749 individuals with unexplained intellectual disability (ID) ascertained by the Department of Human Genetics of Radboud University Medical Center (Nijmegen, the Netherlands), and the other was ascertained at the Department of Genetics, University Medical Center Utrecht (Utrecht, the Netherlands). A third individual was identified in a cohort of 1,133 children with severe, undiagnosed developmental disorders through the DDD research variant list on DECIPHER.[18] Additionally, four individuals with *SPOP* variants detected by clinical exome sequencing were identified via GeneMatcher.[19] One girl with ID was referred to the Molecular Diagnostic Laboratory at the University of Chicago for clinical exome sequencing (Chicago, Illinois, USA). The other individuals were selected from a cohort of 14,183 individuals who had neurodevelopmen-

tal disorders and who underwent trio-based clinical exome sequencing at GeneDx (Gaithersburg, Maryland, USA). All legal representatives signed consent to share medical information and clinical photographs, and this study was approved by the institutional review board Commissie Mensgebonden Onderzoek Regio Arnhem-Nijmegen under CMO approval number NL36191.091.11.

Six unique *de novo* missense variants in *SPOP* (GenBank: NM_001007226.1) were identified in peripheral blood of these seven individuals with intellectual disability: c.73A>G, p.Thr25Ala; c.248A>G, p.Tyr83Cys; c.362G>A, p.Arg121Gln; c.395G>T, p.Gly132Val; a recurrent c.412C>T, p.Arg138Cys; and c.430G>A, p.Asp144Asn (Figure 1; Tables 1 and 2; Table S1). All variants were confirmed by Sanger sequencing. With the exception of p.Thr25Ala, which is positioned six amino acids before the start of the MATH domain, all variants were located within the MATH domain. Three of these variants are identical to those described in cancers of the prostate, endometrium, lung, and large intestine (Table S2). *In silico* analyses, which we performed to assess evolutionary constraints on SPOP, showed that all affected amino acids are fully

Table 1. De Novo Likely Pathogenic Variants in SPOP

Location	cDNA Change [a,c]	Amino Acid Change [b,c]	Mutation Type	CADD Score	Domain	Predicted Effect on the Protein [28–30,d]	Affected Individuals
Exon 5	c.73A>G	p.Thr25Ala	missense	26.0	not in a domain	disease causing	individual 4
Exon 7	c.248A>G	p.Tyr83Cys	missense	25.6	MATH	disease causing	individual 7
Exon 8	c.362G>A	p.Arg121Gln	missense	32	MATH	disease causing	individual 1
Exon 8	c.395G>T	p.Gly132Val	missense	32	MATH	disease causing	individual 3
Exon 8	c.412C>T	p.Arg138Cys	missense	28.3	MATH	disease causing	individuals 5 and 6
Exon 8	c.430G>A	p.Asp144Asn	missense	28.9	MATH	disease causing	individual 2

[a]GenBank: NM_001007226.1.
[b]GenBank: NP_001007227.1.
[c]None of these *SPOP* variants were identified in the gnomAD.
[d]With the exception of p.Arg121Gln, which was predicted to be benign by PolyPhen-2, all variants were predicted to be disease causing by SIFT (v. 6.2.0), Mutation Taster (v2013), and PolyPhen-2.

conserved down to *C. elegans* (Figure S1). None of the variants were reported in the Genome Aggregation Database (gnomAD),[20] and the CADD (combined annotation-dependent depletion) score[21] was higher than 25 for all variants. In ExAC,[20] *SPOP* contains fewer missense variants than expected (Z score = 4.74), and no loss of function variant is described (pLi = 0.99). In the DGV (Database of Genomic Variants; March 2019),[22] no CNVs, inversions, or indels were reported. We used MetaDome[23,24] to generate a tolerance landscape, which is a regional tolerance plot for genetic variation and is based on the ratio of observed missense and synonymous (d_N/d_S) variants that are included in gnomAD r2.0[20] and are found in the protein-coding region of *SPOP*. All *de novo* SPOP variants are located in regions that are extremely intolerant to missense variants (Figure S2). We investigated the 3D location of the variants by using the experimentally solved 3D-conformation of the dimeric SPOP structure (PDB file 3hqi; Figure 2A).[25] The structure was analyzed with the YASARA and WHAT IF Twinset.[26,27] This analysis suggested that four of the six substitutions, p.Tyr83Cys, p.Arg121Gln, p.Gly132Val, and p.Arg138Cys, would directly affect the binding of substrates to SPOP. For the p.Asp144Asn and p.Thr25Ala variants, prediction of the binding consequences was non-informative. The p.Asp144Asn substitution was not predicted to have a large effect on the local protein structure, and residue Thr 25 is too distant from the binding cleft.

Reverse deep phenotyping of the seven individuals revealed that all had intellectual disability, motor and speech delay, facial dysmorphisms, and congenital anomalies (Table 2; Table S3; Figure 1; Figure S3). Besides these common features, individuals 1 and 2 shared craniofacial dysmorphisms that are strikingly different from those of individuals 3–7; in fact, when one considers the head circumference and forehead of individuals 1 and 2, their craniofacial dysmorphisms could even be said to be the opposite of the features of individuals 3–7. Individuals 1 and 2 both presented with specific features that include congenital microcephaly, hearing loss, and a recognizable facial gestalt, such as a small forehead, highly arched eyebrows, blepharophimosis, a full nasal tip, a flat philtrum, micrognathia, and a pointed chin. Between them, individuals 3–7 also shared specific facial dysmorphisms, in particular (relative) macrocephaly, a high and broad forehead, and hypertelorism. Additional overlapping phenotypic abnormalities confined to the second group of five individuals were failure to thrive and short stature (2/5), cardiovascular abnormalities (4/4), endocrine abnormalities (3/4), epilepsy (2/4), and sleep disturbance (4/5).

On the basis of the previously reported opposite functional effect of somatic *SPOP* variants in prostate and endometrial cancer (Table S2),[10] we hypothesized that the divergent phenotype of the two groups of individuals corresponds to differential functional effects. We envisaged that the *de novo* variants, including p.Arg121Gln, that were identified in the first group of individuals would result in a gain-of-function, and conversely, the variants, namely p.Tyr83Cys, that were detected in the second group would have a dominant-negative effect. To investigate this, we measured BET protein amounts in human Ishikawa endometrial cancer cells, an isogenic model system, in which we introduced all *de novo* SPOP variants. Variants p.Arg121Gln and p.Asp144Asn resulted in reduced amounts of the BET proteins BRD2, BRD3, and BRD4, suggesting that these are gain-of-function variants comparable to those seen in endometrial cancer (Figures 2B, S4A, and S5). In contrast, the variants p.Thr25Ala, p.Tyr83Cys, p.Gly132Val, and p.Arg138Cys resulted in an upregulation of BRD2, BRD3, and BRD4 protein amounts and are hence *SPOP* variants such as those seen in prostate cancer and are acting in a dominant-negative manner. Importantly, and in conjunction with the notion of altered protein stability, we did not observe relevant transcriptional changes in BET proteins in response to these mutants (Figure S4B). We confirmed the nature of the variants by measuring the kinetics of protein degradation by using two variants that represent either gain-of-function or dominant-negative effects. Indeed, after inhibition of protein synthesis with cycloheximide, BET amounts remained

Table 2. Genotype and Phenotype of Individuals with *De Novo* Pathogenic Mutations in *SPOP*

	Individuals		Individuals				
	1	**2**	**3**	**4**	**5**	**6**	**7**
Gender/ Current age	F; 4 years 7 months	M; 10 years	F; 10 months	M; 17 years 11 months	M; 17 years 9 months	F; 20 years	F; 15 years
Genotype							
cDNA change [a]	c.362G>A	c.430G>A	c.395G>T	c.73A>G	c.412C>T	c.412C>T	c.248A>G
Protein change [b]	p.Arg121Gln	p.Asp144Asn	p.Gly132Val	p.Thr25Ala	p.Arg138Cys	p.Arg138Cys	p.Tyr83Cys
Inheritance	*de novo*	*de novo*	*de novo*	*de novo*	*de novo*	*de novo*	*de novo*
Effect on BET proteins	gain-of-function	gain-of-function	loss-of-function	loss-of-function	loss-of-function	loss-of-function	loss-of-function
Phenotype[d]							
Age at measurements	4 years 7 months	16 months	10 months	17 years 11 months	17 years 9 months	20 years	15 years
Height in cm (centile range)[c]	104.5 cm (~50th)	77 cm (10th–25th)	65.1 cm (−2.5SD)	151.8 cm (−3.1SD)	178.5 cm (50th–75th)	172 cm (90th–97th)	158.8 cm (25th–50th)
Weight in kg (centile range)[c]	15.3 kg (10th–25th)	8.8 kg (−2.3 SD)	5.6 kg (−4 SD)	49.7 kg (3rd)	73 kg (50th–75th)	89 kg (97th)	90.7 kg (+2.5 SD)
HC in cm (centile range)[c]	44 cm (−4 SD)	40.5 cm (−5 SD)	49 cm (+3.5 SD)	NA (25th)	56.4 cm (75th–90th)	57 cm (+2.5 SD)	56 cm at 5 years (+4 SD)
Intellectual disability/ developmental delay[d]	+ (mild)	+ (severe)	+	+ (IQ = 46)	+ (IQ = 45)	+ (IQ = 53)	+ (mild)
Epilepsy	−	NA	−	+	+	NA	−
Behavioral abnormalities[d]	+	+	NA	+	+	+	+
Craniofacial dysmorphims[d]	++	++	+	+	+	+	+
Hearing impairment[d]	+	+	−	−	−	−	−
Cardiovascular abnormality[d]	−	−	+	+	NA	+	+
Endocrine abnormality[d]	−	−	−	+	+	NA	+
Sleep disturbance[d]	−	NA	−	+	+	+	+

Abbreviations are as follows: +, present; −, absent; F, female; M, male; SD, standard deviation; HC, head circumference; IQ, intelligence quotient score; and NA, not available.
[a]GenBank:NM_001007226.1.
[b]GenBank: NP_001007227.1.
[c]Percentile range; if the percentile is <3rd or >97th, standard deviation (SD) is indicated.
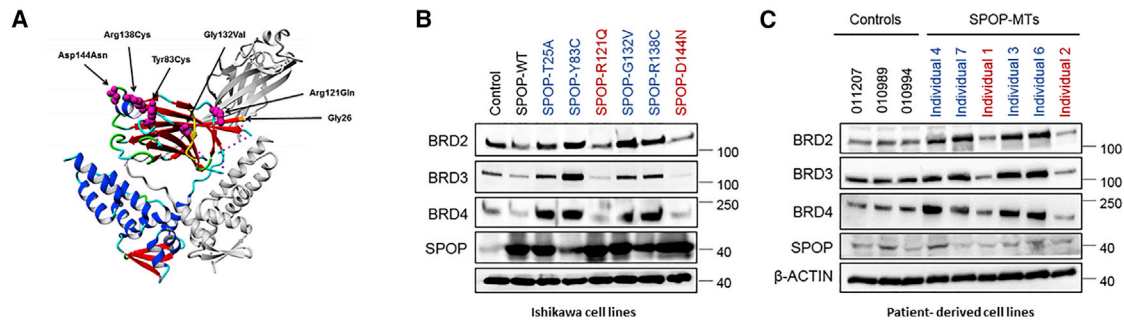[d]Further specified in Table S2

Figure 2. *De Novo SPOP* Variants Produce Opposing Effects on BET Amounts

(A) 3D structure of an asymmetric homodimer SPOP (one monomer is shown in grey), including the MATH domain (most beta strands are in the upper part of the protein and are shown as red arrows) and the BTB domain (blue helices and three beta strands on the lower part). Except for variant p.Thr25Ala, tered residues (magenta spheres) occurred in the MATH domain. The p.Thr25Ala residue is not shown because the protein structure starts with residue 26 (orange extremity of a red beta strand). The displayed mutated residues are closely located to the binding cleft, where the MATH domain interacts with its substrates (yellow peptide). The structure shows that Gly 132 is located at the bottom of the binding cleft, where the introduction of a larger valine affects the conformation and modifies substrate interaction. Tyr 83, Arg 138, and Asp 144 can be found clustered together on the surface of the protein. The alteration of both Tyr 83 and Arg 138 into a cysteine is very likely to affect the local structure surrounding the binding cleft and, hence, disturb SPOP substrate interaction. The substitution of an Asp for an Asn at position 144 is not large enough to affect the structure in a similar way, so we cannot predict the effect of this substitution for now. Amino acid residue Arg 121 is located on the protein surface on the opposite side of the binding cleft, where its side chain supports Tyr 123. Changing this residue to a slightly smaller Gln could affect the position of Tyr 123 and change the interaction of SPOP with its substrate. Lastly, Thr 25 is even more distant from the binding cleft. This residue is not present in the PDB file, but because Gly 26 is present as the first residue of the solved protein chain, we could still infer the effect of this change. The change of a Thr into a smaller Ala is not expected to cause strong structural changes or to affect the binding site directly.

(B) Representative immunoblot showing that the p.Asp144Asn and p.Arg121Gln SPOP substitutions downregulate, whereas p.Thr25Ala, p.Tyr83Cys, p.Gly132Val, and p.Arg138Cys upregulate, BRD2, BRD3, and BRD4 protein amounts when compared with wild-type SPOP (SPOP-WT) in Ishikawa endometrial cancer cells.

(C) When proband-derived Epstein-Barr Virus (EBV)-immortalized PBMC lines from individuals 1, 2, 3, 4, 6, and 7 were compared to cell lines from three healthy individuals (controls), the same effect as for the isogenic cells (in B) was observed. β-ACTIN was used as loading control. Molecular weights are indicated (kDa).

stable upon expression of SPOP-p.Arg138Cys. In contrast, protein half-life was more dramatically reduced upon expression of SPOP-p.Asp144Asn as compared to that of wild-type SPOP (Figure S6). Consistent with the notion that BETs are degraded through the proteasome, treatment with MG132 restored BET amounts in both contexts. Proband-derived EBV-immortalized peripheral blood mononuclear cell (PBMC) lines from individuals 1, 2, 3, 4, 6, and 7 were additionally obtained and cultured as previously described.[31] Notably, measurements of BET amounts in proband-derived cell lines matched those found in healthy individuals in terms of the deregulation found in the isogenic system generated in Ishikawa endometrial cancer cells (Figures 2B, 2C, and S4C), suggesting that the *de novo* variants are causally linked to the functional effects observed.

We identified seven individuals with NDD and *de novo SPOP* missense variants that caused either reduced (individuals 1 and 2) or increased (individuals 3–7) BET amounts. Furthermore, variants resulted in growth abnormalities, including a head size spectrum ranging from microcephaly to macrocephaly and distinct recognizable facial dysmorphisms. Whereas individuals with gain-of-function variants presented with microcephaly, individuals with variants leading to BET's functional loss had absolute macrocephaly or a head circumference (HC) in the normal centile range, though exceeding the centile for height (relative macrocephaly). Of note, individuals 5 and 6, who had the same *de novo* p.Arg138Cys variant, had absolute macroce-

phaly and a normal HC, respectively, suggesting interfamilial variability. So far, no true congenital macrocephaly has been observed, although birth HC measurements of individuals 5, 6, and 7 were unknown. Specifically, individuals 3 and 4, who were born with below average HC, showed postnatal ventriculomegaly, which also contributed to absolute or relative macrocephaly, respectively. Additional investigation is needed if we are to understand the intricate mechanisms involved in head growth in individuals with pathogenic *SPOP* variants; such mechanisms might be determined by cell signaling pathways that govern cell proliferation and overlap with cancer pathways.[32] Functionally, BET proteins are involved in cell-cycle progression.[33] In mice, BRD2, BRD3, and BRD4 were found to be downregulated in differentiating neural progenitor cells, whereas their amounts remained unaltered in proliferating neural progenitor cells.[34] In addition, in *Brd2*-deficient neuroepithelial cells, cell-cycle progression was accelerated, whereas neuronal differentiation as well as cell-cycle exit were impaired.[35] These results correlate well with the congenital microcephaly found in two individuals with a STOP gain of function resulting in fewer BET proteins and, hence, supposedly less neuronal differentiation. Conversely, more BET proteins would stimulate the latter process, which might result in macrocephaly. Lastly, a c.910C>T (p.His304Tyr; GenBank: NM_058243.2) heterozygous missense variant in *BRD4* has been described as resulting in macrocephaly and short stature, resembling

features in individuals with dominant-negative variants in SPOP.[36] Interestingly, this BRD4 variant might result in increased protein stability because it is in close proximity to the SPOP degron (AA292–299).

Diverse and eventually mirror phenotypes caused by genetic variation in the same gene are increasingly recognized (e.g. CDKN1C[37] and RAC1[38]). Different explanations that have been proposed for the resultant excess or inhibition of cell proliferation and differentiation include disruption of a single neurodevelopmental step that is sensitive to gene dosage[39] and the possibility of a gene's influencing several biologic pathways resulting in different consequences depending on temporal and cellular contexts within a genetic background.[1] In particular, the (re)occurrence of specific genetic variants in the substrate-binding MATH domain of SPOP, which results in opposite functional effects, emphasizes the key role of this domain in cell biology.

In summary, SPOP variants have been identified in individuals with intellectual disability and in tumor samples, which suggests that SPOP variants occurring at different times of development, specifically in germline versus somatic tissue, result in different consequences, i.e., neurodevelopmental delay or cancer, respectively. Individuals with NDD and de novo SPOP variants could be differentiated on the basis of distinct craniofacial dysmorphisms and congenital anomalies, indicating the presence of diverse clinically recognizable intellectual-disability syndromes. The opposing effects of variants impairing SPOP function provide a molecular basis for the contrasting phenotypic differences.

Supplemental Data

Supplemental Data can be found online at https://doi.org/10.1016/j.ajhg.2020.02.001.

Web Resources

Genome Aggregation Database, https://gnomad.broadinstitute.org/gene/ENSG00000121067

OMIM, https://www.omim.org/

References

1. Hoischen, A., Krumm, N., and Eichler, E.E. (2014). Prioritization of neurodevelopmental disease genes by discovery of new mutations. Nat. Neurosci. 17, 764–772.

2. Tartaglia, M., Kalidas, K., Shaw, A., Song, X., Musat, D.L., van der Burgt, I., Brunner, H.G., Bertola, D.R., Crosby, A., Ion, A., et al. (2002). PTPN11 mutations in Noonan syndrome: molecular spectrum, genotype-phenotype correlation, and phenotypic heterogeneity. Am. J. Hum. Genet. 70, 1555–1563.

3. Tartaglia, M., Niemeyer, C.M., Fragale, A., Song, X., Buechner, J., Jung, A., Hählen, K., Hasle, H., Licht, J.D., and Gelb, B.D. (2003). Somatic mutations in PTPN11 in juvenile myelomonocytic leukemia, myelodysplastic syndromes and acute myeloid leukemia. Nat. Genet. 34, 148–150.

4. Gelsi-Boyer, V., Trouplin, V., Adélaïde, J., Bonansea, J., Cervera, N., Carbuccia, N., Lagarde, A., Prebet, T., Nezri, M., Sainty, D., et al. (2009). Mutations of polycomb-associated gene ASXL1 in myelodysplastic syndromes and chronic myelomonocytic leukaemia. Br. J. Haematol. 145, 788–800.

5. Hoischen, A., van Bon, B.W., Rodríguez-Santiago, B., Gilissen, C., Vissers, L.E., de Vries, P., Janssen, I., van Lier, B., Hastings, R., Smithson, S.F., et al. (2011). De novo nonsense mutations in ASXL1 cause Bohring-Opitz syndrome. Nat. Genet. 43, 729–731.

6. Carbuccia, N., Murati, A., Trouplin, V., Brecqueville, M., Adélaïde, J., Rey, J., Vainchenker, W., Bernard, O.A., Chaffanet, M., Vey, N., et al. (2009). Mutations of ASXL1 gene in myeloproliferative neoplasms. Leukemia 23, 2183–2186.

7. Cheng, J., Guo, J., Wang, Z., North, B.J., Tao, K., Dai, X., and Wei, W. (2018). Functional analysis of Cullin 3 E3 ligases in tumorigenesis. Biochim Biophys Acta Rev Cancer 1869, 11–28.

8. Nagai, Y., Kojima, T., Muro, Y., Hachiya, T., Nishizawa, Y., Wakabayashi, T., and Hagiwara, M. (1997). Identification of a novel nuclear speckle-type protein, SPOP. FEBS Lett. 418, 23–26.

9. Zapata, J.M., Pawlowski, K., Haas, E., Ware, C.F., Godzik, A., and Reed, J.C. (2001). A diverse family of proteins containing tumor necrosis factor receptor-associated factor domains. J. Biol. Chem. 276, 24242–24252.

10. Janouskova, H., El Tekle, G., Bellini, E., Udeshi, N.D., Rinaldi, A., Ulbricht, A., Bernasocchi, T., Civenni, G., Losa, M., Svinkina, T., et al. (2017). Opposing effects of cancer-type-specific SPOP mutants on BET protein degradation and sensitivity to BET inhibitors. Nat. Med. 23, 1046–1054.

11. Baca, S.C., Prandi, D., Lawrence, M.S., Mosquera, J.M., Romanel, A., Drier, Y., Park, K., Kitabayashi, N., MacDonald, T.Y., Ghandi, M., et al. (2013). Punctuated evolution of prostate cancer genomes. Cell 153, 666–677.

12. Barbieri, C.E., Baca, S.C., Lawrence, M.S., Demichelis, F., Blattner, M., Theurillat, J.P., White, T.A., Stojanov, P., Van Allen, E.,

Stransky, N., et al. (2012). Exome sequencing identifies recurrent SPOP, FOXA1 and MED12 mutations in prostate cancer. Nat. Genet. *44*, 685–689.

13. Le Gallo, M., O'Hara, A.J., Rudd, M.L., Urick, M.E., Hansen, N.F., O'Neil, N.J., Price, J.C., Zhang, S., England, B.M., Godwin, A.K., et al.; NIH Intramural Sequencing Center (NISC) Comparative Sequencing Program (2012). Exome sequencing of serous endometrial tumors identifies recurrent somatic mutations in chromatin-remodeling and ubiquitin ligase complex genes. Nat. Genet. *44*, 1310–1315.

14. Geng, C., He, B., Xu, L., Barbieri, C.E., Eedunuri, V.K., Chew, S.A., Zimmermann, M., Bond, R., Shou, J., Li, C., et al. (2013). Prostate cancer-associated mutations in speckle-type POZ protein (SPOP) regulate steroid receptor coactivator 3 protein turnover. Proc. Natl. Acad. Sci. USA *110*, 6997–7002.

15. Theurillat, J.P., Udeshi, N.D., Errington, W.J., Svinkina, T., Baca, S.C., Pop, M., Wild, P.J., Blattner, M., Groner, A.C., Rubin, M.A., et al. (2014). Prostate cancer. Ubiquitylome analysis identifies dysregulation of effector substrates in SPOP-mutant prostate cancer. Science *346*, 85–89.

16. An, J., Ren, S., Murphy, S.J., Dalangood, S., Chang, C., Pang, X., Cui, Y., Wang, L., Pan, Y., Zhang, X., et al. (2015). Truncated ERG Oncoproteins from TMPRSS2-ERG Fusions Are Resistant to SPOP-Mediated Proteasome Degradation. Mol. Cell *59*, 904–916.

17. Marzahn, M.R., Marada, S., Lee, J., Nourse, A., Kenrick, S., Zhao, H., Ben-Nissan, G., Kolaitis, R.M., Peters, J.L., Pounds, S., et al. (2016). Higher-order oligomerization promotes localization of SPOP to liquid nuclear speckles. EMBO J. *35*, 1254–1275.

18. Deciphering Developmental Disorders, S.; and Deciphering Developmental Disorders Study (2015). Large-scale discovery of novel genetic causes of developmental disorders. Nature *519*, 223–228.

19. Sobreira, N., Schiettecatte, F., Valle, D., and Hamosh, A. (2015). GeneMatcher: a matching tool for connecting investigators with an interest in the same gene. Hum. Mutat. *36*, 928–930.

20. Lek, M., Karczewski, K.J., Minikel, E.V., Samocha, K.E., Banks, E., Fennell, T., O'Donnell-Luria, A.H., Ware, J.S., Hill, A.J., Cummings, B.B., et al.; Exome Aggregation Consortium (2016). Analysis of protein-coding genetic variation in 60,706 humans. Nature *536*, 285–291.

21. Kircher, M., Witten, D.M., Jain, P., O'Roak, B.J., Cooper, G.M., and Shendure, J. (2014). A general framework for estimating the relative pathogenicity of human genetic variants. Nat. Genet. *46*, 310–315.

22. MacDonald, J.R., Ziman, R., Yuen, R.K., Feuk, L., and Scherer, S.W. (2014). The Database of Genomic Variants: a curated collection of structural variation in the human genome. Nucleic Acids Res. *42*, D986–D992.

23. Wiel, L., Baakman, C., Gilissen, D., Veltman, J.A., Vriend, G., and Gilissen, C. (2019). MetaDome: Pathogenicity analysis of genetic variants through aggregation of homologous human protein domains. Hum. Mutat. *40*, 1030–1038.

24. Wiel, L., Venselaar, H., Veltman, J.A., Vriend, G., and Gilissen, C. (2017). Aggregation of population-based genetic variation over protein domain homologues and its potential use in genetic diagnostics. Hum. Mutat. *38*, 1454–1463.

25. Zhuang, M., Calabrese, M.F., Liu, J., Waddell, M.B., Nourse, A., Hammel, M., Miller, D.J., Walden, H., Duda, D.M., Seyedin, S.N., et al. (2009). Structures of SPOP-substrate complexes: insights into molecular architectures of BTB-Cul3 ubiquitin ligases. Mol. Cell *36*, 39–50.

26. Krieger, E., Koraimann, G., and Vriend, G. (2002). Increasing the precision of comparative models with YASARA NOVA–a self-parameterizing force field. Proteins *47*, 393–402.

27. Vriend, G. (1990). WHAT IF: a molecular modeling and drug design program. J. Mol. Graph *8*, 52–56.

28. Sim, N.L., Kumar, P., Hu, J., Henikoff, S., Schneider, G., and Ng, P.C. (2012). SIFT web server: predicting effects of amino acid substitutions on proteins. Nucleic Acids Res. *40*, W452–W457.

29. Adzhubei, I.A., Schmidt, S., Peshkin, L., Ramensky, V.E., Gerasimova, A., Bork, P., Kondrashov, A.S., and Sunyaev, S.R. (2010). A method and server for predicting damaging missense mutations. Nat. Methods *7*, 248–249.

30. Schwarz, J.M., Cooper, D.N., Schuelke, M., and Seelow, D. (2014). MutationTaster2: mutation prediction for the deep-sequencing age. Nat. Methods *11*, 361–362.

31. de Brouwer, A.P., van Bokhoven, H., and Kremer, H. (2006). Comparison of 12 reference genes for normalization of gene expression levels in Epstein-Barr virus-transformed lymphoblastoid cell lines and fibroblasts. Mol. Diagn. Ther. *10*, 197–204.

32. Pirozzi, F., Nelson, B., and Mirzaa, G. (2018). From microcephaly to megalencephaly: determinants of brain size. Dialogues Clin. Neurosci. *20*, 267–282.

33. Doroshow, D.B., Eder, J.P., and LoRusso, P.M. (2017). BET inhibitors: a novel epigenetic approach. Ann. Oncol. *28*, 1776–1787.

34. Li, J., Ma, J., Meng, G., Lin, H., Wu, S., Wang, J., Luo, J., Xu, X., Tough, D., Lindon, M., et al. (2016). BET bromodomain inhibition promotes neurogenesis while inhibiting gliogenesis in neural progenitor cells. Stem Cell Res. (Amst.) *17*, 212–221.

35. Tsume, M., Kimura-Yoshida, C., Mochida, K., Shibukawa, Y., Amazaki, S., Wada, Y., Hiramatsu, R., Shimokawa, K., and Matsuo, I. (2012). Brd2 is required for cell cycle exit and neuronal differentiation through the E2F1 pathway in mouse neuroepithelial cells. Biochem. Biophys. Res. Commun. *425*, 762–768.

36. Jin, H.S., Kim, J., Kwak, W., Jeong, H., Lim, G.B., and Lee, C.G. (2017). Identification of a Novel Mutation in BRD4 that Causes Autosomal Dominant Syndromic Congenital Cataracts Associated with Other Neuro-Skeletal Anomalies. PLoS ONE *12*, e0169226.

37. Milani, D., Pezzani, L., Tabano, S., and Miozzo, M. (2014). Beckwith-Wiedemann and IMAGe syndromes: two very different diseases caused by mutations on the same gene. Appl. Clin. Genet. *7*, 169–175.

38. Reijnders, M.R.F., Ansor, N.M., Kousi, M., Yue, W.W., Tan, P.L., Clarkson, K., Clayton-Smith, J., Corning, K., Jones, J.R., Lam, W.W.K., et al.; Deciphering Developmental Disorders Study (2017). RAC1 Missense Mutations in Developmental Disorders with Diverse Phenotypes. Am. J. Hum. Genet. *101*, 466–477.

39. Jacquemont, S., Reymond, A., Zufferey, F., Harewood, L., Walters, R.G., Kutalik, Z., Martinet, D., Shen, Y., Valsesia, A., Beckmann, N.D., et al. (2011). Mirror extreme BMI phenotypes associated with gene dosage at the chromosome 16p11.2 locus. Nature *478*, 97–102.